

6
-12-75

Dr - 1194

UCRL-51737

**HYDROGEN-ISOTOPE FLOW
IN THE ROTATING-TARGET NEUTRON SOURCE**

R. A. Nickerson

January 15, 1975

MASTER

Prepared for U.S. Atomic Energy Commission under contract No. W-7405-Eng-48



**LAWRENCE
LIVERMORE
LABORATORY**

University of California / Livermore

DISTRIBUTION OF THIS DOCUMENT IS UNLIMITED

NOTICE

"This report was prepared as an account of work sponsored by the United States Government. Neither the United States nor the United States Atomic Energy Commission, nor any of their employees, nor any of their contractors, subcontractors, or their employees, makes any warranty, express or implied, or assumes any legal liability or responsibility for the accuracy, completeness or usefulness of any information, apparatus, product or process disclosed, or represents that its use would not infringe privately-owned rights."

Printed in the United States of America
Available from
National Technical Information Service
U. S. Department of Commerce
5285 Port Royal Road
Springfield, Virginia 22151
Price: Printed Copy \$ ____; Microfiche \$1.45

<u>* Pages</u>	<u>NTIS Selling Price</u>
1-50	\$4.00
51-150	\$5.45
151-325	\$7.60
326-500	\$10.60
501-1000	\$13.60



LAWRENCE LIVERMORE LABORATORY
University of California, Livermore, California, 94550

UCRL-51737

HYDROGEN-ISOTOPE FLOW IN THE ROTATING-TARGET NEUTRON SOURCE

R. A. Nickerson

MS. Date: January 15, 1975

NOTICE

This report was prepared as an account of work sponsored by the United States Government. Neither the United States nor the United States Energy Research and Development Administration, nor any of their employees, nor any of their contractors, subcontractors, or their employees, makes any warranty, express or implied, or assumes any legal liability or responsibility for the accuracy, completeness or usefulness of any information, apparatus, product or process disclosed, or represents that its use would not infringe privately owned rights.

MASTER

RECEIVED ...
JAN 21 1975
JAN 21 1975

Contents

Abstract	1
Introduction	1
Operating Characteristics	1
The Diffusion of Hydrogen Isotopes in Titanium	3
Mass Transport in the Rotating Target	4
Results of the Mass-Flow Study	6
Initial Test Cases	6
Parametric Design Study	8
Conclusions	12
References	13

HYDROGEN-ISOTOPE FLOW IN THE ROTATING-TARGET NEUTRON SOURCE

Abstract

The degradation mechanisms of titanium tritide (TiT_2) neutron-source targets are not completely understood. Mass flow of the target tritium and the beam-implanted deuterium under rapidly pulsed heat fluxes of rotating targets have not been investigated. This report presents results of mass-flow calculations using the TRUMP heat-flow finite-difference

computer code. The conclusion of this study is that the best compromise between long target life and high neutron output is achieved when targets are operated in the narrow range where the rate of evolution of hydrogen isotopes from the target just balances the rate of deposition of hydrogen isotopes from the beam.

Introduction

The target presently in use in the Insulated Core Transformer (ICT) accelerator is described as a 0.01-mm titanium tritide layer on a 1-mm-thick, 150-mm-o. d. Amzirc disk rotating at 115.2 rad/s (1100 rpm) with 3.15×10^{-4} m³/s (5 gpm) of cooling water.¹ This target produces 2×10^{12} neutrons per second with 10 mA of deuteron current at 400 keV and falls to one half of this rate in about 100 h of target operation.

Current efforts to increase target output are concerned with dissipation of

the higher heat fluxes of increased beam currents. This effort is directed at larger targets rotating faster, with improved water-cooling procedures [330 mm o. d. at 576 rad/s (5500 rpm) in air bearings with 6.30×10^{-4} m³/s (10 gpm) of cooling water].

This note is a further consideration of the details of the degradation mechanisms in the titanium hydride target layer. It considers mass movement of the tritium and implanted deuterium in the titanium under the influence of the pulsed heat flux.

Operating Characteristics

Logan² makes the following observations and calculations to describe the target operating characteristics:

- a. The tritium content of a new target approaches 1.5 tritium atoms per atom of titanium. The fully stoichiometric

compound TiT_2 has a tritium-atom density twice that of liquid tritium at 20 K.

b. The target, because of its rotation, is subjected to a repeating cycle of a rapid temperature rise as it rotates through the beam, a rapid quench as it conducts heat to the copper backing, and a gradual cooling as it rotates around to the beam spot again. Two cases were chosen for study as representing extremes of high and low energy densities; these are illustrated in Figs. 1 and 2.

c. The bombarding deuterons lose energy to electrons as they move through target material and come to rest at a

depth of about 17 g/m^2 . An estimate of the implanted (before diffusion) distribution has been made. About 1 deuteron in 3×10^5 reacts with a tritium atom to create a 14-MeV neutron. The burn-up of tritium is also negligible (1 tritium atom in 3×10^5 available tritium atoms per 100 h). Thus, in about 100 h (1 "half-life"), deuterons are implanted in an amount comparable to the original tritium inventory in the reaction region. Figure 3 shows the reaction region for neutrons, the implantation region for unreacted deuterons, and the damage region from ion bombardment.

As a result of these observations, questions immediately arise as to mass transport. It is observed that between

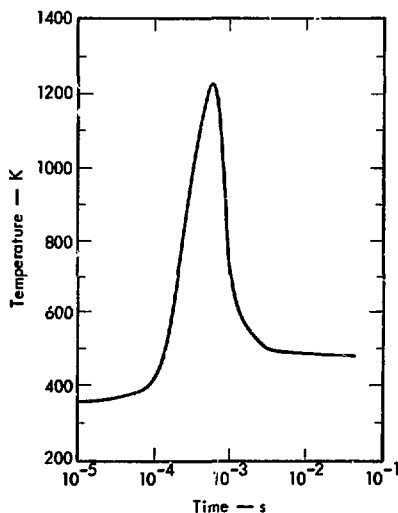


Fig. 1. Calculated temperature-time history at the surface of a TiT_2 -coated copper target for a small (high-energy-density) beam at 6 kW with a beam diameter of 3 mm (FWHM) and a target speed through the beam of 5120 mm/s (45-mm radius at 115.2 rad/s).

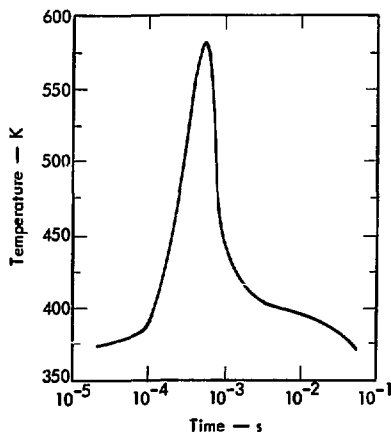


Fig. 2. Calculated temperature-time history at the surface of a TiT_2 -coated copper target for a large (low-energy-density) beam at 6 kW with a beam diameter of 6 mm (FWHM) and a target speed through the beam of 11500 mm/s (100-mm radius at 115.2 rad/s).

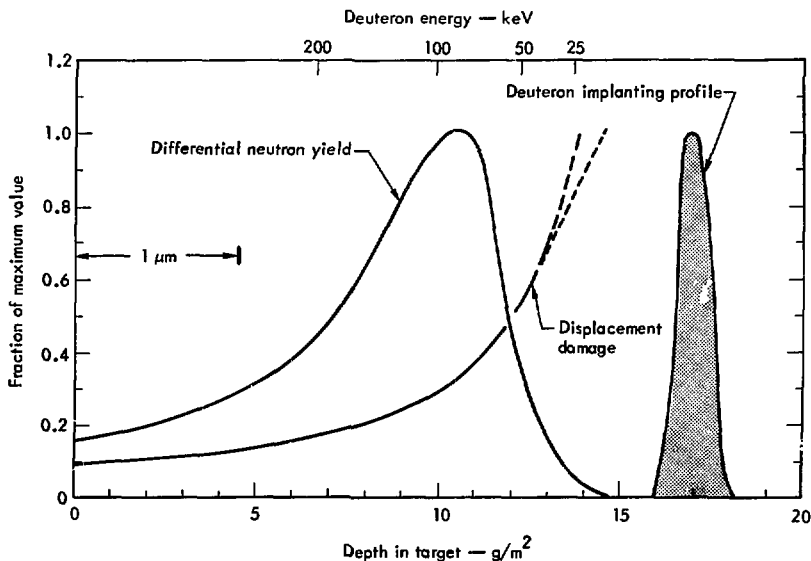


Fig. 3. Neutron yield, displacement damage, and implantation versus distance from target surface for 400-keV deuterons.

0.1 and 0.2 tritium atom per incident deuteron appears in the vacuum pumping system. Surface depletion has been observed; the roles of surface oxides and impurities have been investigated. The depletion of tritium in the region of the deuteron range (the implantation region

of Fig. 3) has been confirmed.³ Many questions remain unanswered, however, and the motion of deuterium and tritium in the target remains as a rather cloudy picture.

The purpose of this investigation was to clarify these questions.

The Diffusion of Hydrogen Isotopes in Titanium

Sandia researchers⁴ considered both theoretically and experimentally the decomposition of a TiH₂ coupon 0.38 mm (0.015 in.) thick at 523, 673, and 773 K. First they calculated the decomposition rate based upon proper choice of phases present at each temperature and the

change of concentration (phase boundary movement) as solid-state diffusion progressed. They then experimentally measured the decomposition rate. These findings are presented in Fig. 4.

Their conclusion is as follows: "A comparison of the computed decomposition

rate based on the diffusion model shows that the observed decomposition rate is many times slower at all temperatures. The slowness of the rate plus the failure to obtain a linear relation with \sqrt{t} implies that the rate is not controlled by diffusion of hydrogen in the solid."

They then show that experimentally observed decomposition rates are affected in only a minor way by oxide films. Even anodized surface layers have minimum effect on decomposition rates.

The largest single factor affecting decomposition rate seemed to be the pumping speed and residual chamber pressure in the decomposition chamber. They thus concluded that the surface reactions and back partial pressure of hydrogen at the surface were the rate-controlling factors.

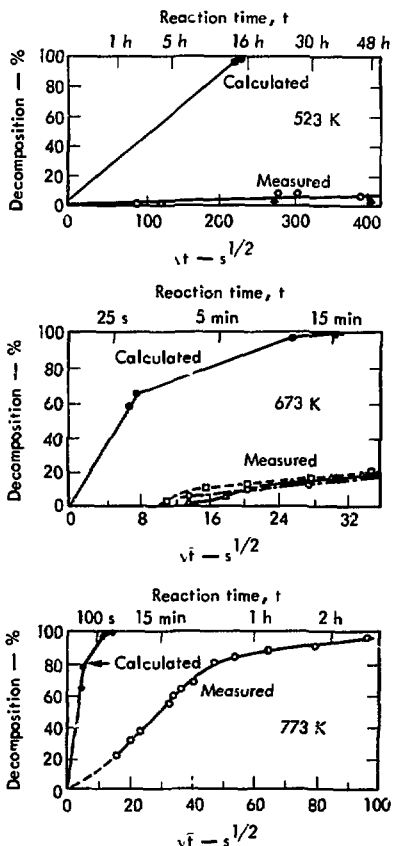


Fig. 4. Decomposition of a 0.38-mm-thick slab of $TiTi_2$ as a function of time at three temperatures: 523 K, 673 K, and 773 K.¹

Mass Transport in the Rotating Target

Logan² used the TRUMP finite-difference code to calculate the temperature distributions of Figs. 1 and 2. This code uses (for one dimension) finite-difference methods to solve the differential equation:

$$\rho C \frac{\partial T}{\partial t} = k \frac{\partial^2 T}{\partial x^2},$$

where

T = temperature,
 t = time,
 ρ = density,
 C = specific heat,
 k = thermal conductivity,
 x = distance.

However, TRUMP is embellished with many features commonly encountered in heat-transfer problems. It can treat heat-generation sources; heat losses through surfaces by conduction, convection, and/or radiation; etc. It is flexible in that zones of different materials with different properties may be functions of time, temperature, or specific properties of other zones.

Fick's law for diffusion (mass transport) is

$$\frac{\partial C}{\partial t} = D \frac{\partial^2 C}{\partial x^2},$$

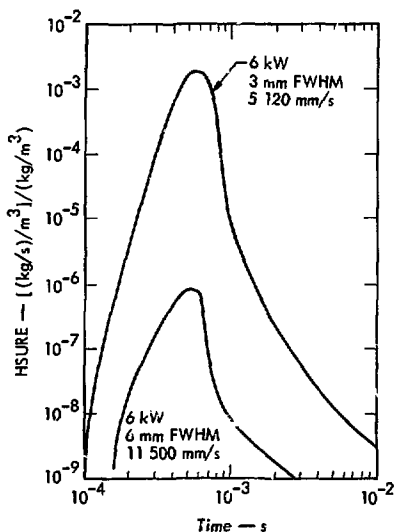


Fig. 5. Time variation of the mass-flow quantity HSURE in the heat-flow code TRUMP. (These curves were obtained from the temperature-time relationships of Figs. 1 and 2 and the Arrhenius equation given on p. 6, which was obtained by modeling the experimental data in Fig. 4 with TRUMP.)

where

C = concentration,
t = time,
D = diffusivity,
x = distance.

TRUMP can also handle mass diffusion as well as the heat diffusion for which it was written. Care must be exercised in the choice of all of the diffusion analogs to the quantities used in the heat-flow case. This presents no difficulties except for the mass-transport flow through a surface.

To resolve this difficulty the experimental data of the Sandia work⁴ was

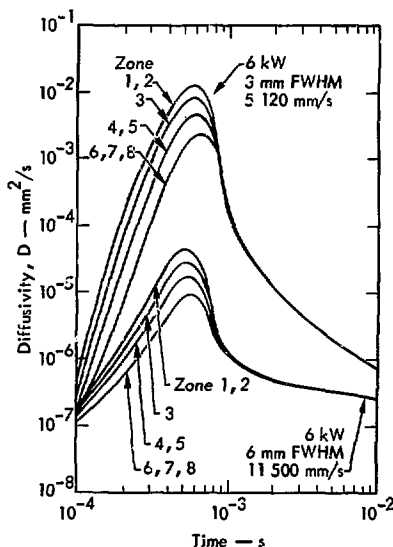


Fig. 6. Time variation of the mass-transport quantity D in the mass-transport equation $\partial C/\partial t = D (\partial^2 C/\partial x^2)$. (These curves were obtained from the temperature-time relationship of Figs. 1 and 2 and the Arrhenius equation given on p. 3.) The TRUMP zone structure is shown in Fig. 8.

used. Their sample was modeled, and a value of TRUMP's quantity HSURE -- the thermal convection coefficient -- was empirically fitted to yield the experimentally measured decomposition rates as a function of temperature. It is recognized that this limits validity to duplication of the experimental conditions of surface-reaction and back-hydrogen-reaction environments. The data, however, is for fairly commonly encountered vacuum levels and pumping rates, and it seems to be the only such data available -- i.e., the only game in town!

The result of this empirical fitting is

$$\text{HSURE} = 1.900 \exp (-71\,044/kT) \text{ s}^{-1},$$

where $k = 8,305 \text{ J/mol} \cdot \text{K}$. Thus, from the temperature-time relationships (Figs. 1 and 2), the HSURE-time relationships can be derived; these are shown in Fig. 5.

The experimental data for the diffusion of hydrogen in titanium is fitted by

$$D = 1.830 \exp (-51\,982/kT) \text{ mm}^2/\text{s},$$

where $k = 8,305 \text{ J/mol} \cdot \text{K}$. This, together with Figs. 1 and 2, yields the diffusivity-time relationship shown in Fig. 6.

Results of the Mass-Flow Study

INITIAL TEST CASES

Figure 7 shows the mass-flow characteristics for the two extreme cases chosen for study (summarized in Table 1). The structure of the TRUMP zones is shown in Fig. 8.

Table 1. Cases illustrated in Fig. 7.

	Power (kW)	Beam profile, FWHM (mm)	Linear velocity through beam (mm/sec)
Fig. 7 (a)	6	3	5 120 (≈ 5 -mm radius at 115.2 rad/s)
Fig. 7 (b)	5	6	11 500 (100-mm radius at 115.2 rad/s)

These cases show two quite different modes of target behavior. The characteristics which distinguish these two modes are delineated below.

First, the higher energy density of the 3-mm (FWHM) beam causes a higher

maximum temperature in the tritide layer. From Fig. 1 this is seen to be about 1223 K. This higher temperature causes the diffusivities to be higher, as seen in Fig. 6 (maximum of $1.15 \times 10^{-2} \text{ mm}^2/\text{s}$). The surface mass transport, HSURE, is correspondingly higher. Because of this higher surface transport and mobility, the loss through the surface per cycle is $3.2 \times 10^{-7} \text{ g}$ of deuterium plus tritium. The deposition rate of deuterium from the beam (at its highest energy density) is $2.38 \times 10^{-9} \text{ g}$ per cycle. Thus, the ratio of rate in to rate out, r_i/r_o , equals 0.0074.

The lower energy density of the 6-mm (FWHM) beam causes a maximum surface temperature of 582 K (Fig. 2). The diffusivity maximum (Fig. 6) is only $3.8 \times 10^{-5} \text{ mm}^2/\text{s}$, and HSURE is correspondingly lower. The result is a lower loss through the surface per cycle, of $1.38 \times 10^{-10} \text{ g}$ of deuterium plus tritium. The deuterium deposition rate (again at its highest energy density) is

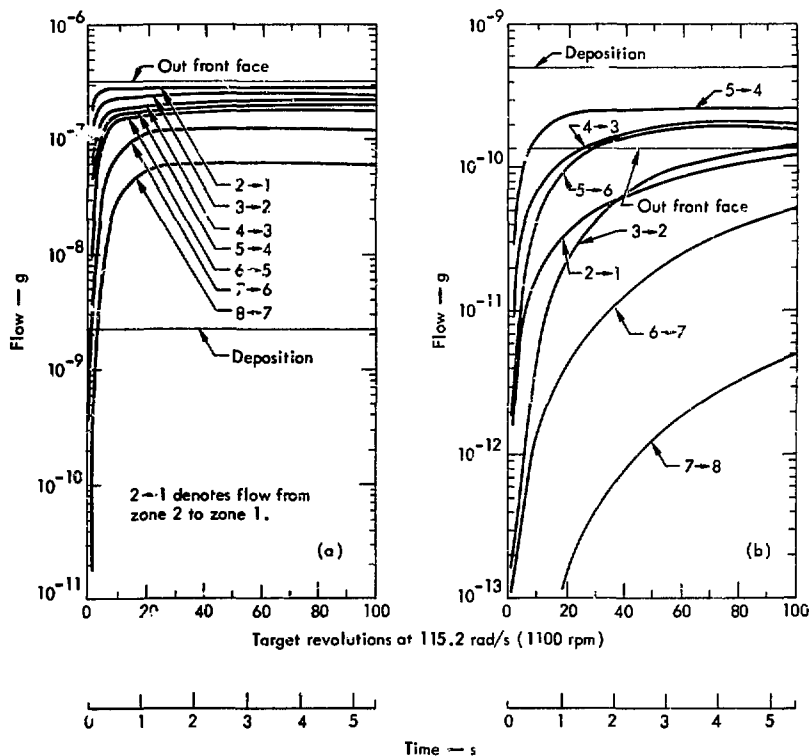


Fig. 7. Mass flow in TiT_2 layer for a 6-kW beam. (a) Beam profile, 3 mm FWHM; linear velocity, 5120 mm/s. (b) Beam profile, 6 mm FWHM; linear velocity, 11500 mm/s. The TRUMP zone structure is shown in Fig. 8.

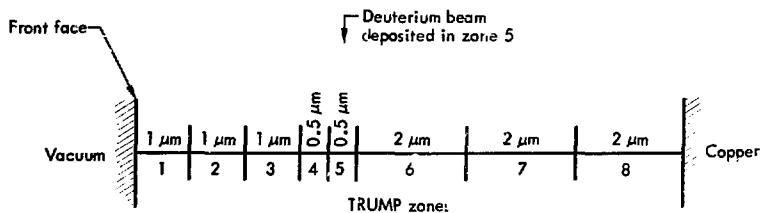


Fig. 8. Zone structure in the TRUMP code.

5.02×10^{-10} g per cycle. Thus $r_i/r_o = 3.64$.

Second, from the mass-flow character of Fig. 7(a) for the high-energy-density beam, we see that mass-flow behavior is completely dominated by the temperature generated by the beam. The relatively low mass-deposition rate does not affect the concentration gradient established by the high temperatures (and thus high diffusivities). The high surface transport rate controls the whole behavior of the target. This loss rate would result in very rapid tritium loss from all zones of the tritide layer and unacceptably short target life.

On the other hand, the mass-flow character of Fig. 7(b) for the low-energy-density beam shows totally different behavior. Here, since the deposition rate is higher than the surface loss rate, the target will fill with increasing time, and the zones behind the deposition zone (zones 6, 7, and 8) will act as a reservoir for deuterium. The tritium contained there cannot have any effect on the neutron production which takes place between the surface and the deuteron range zone (zone 5). Zones 1 to 4 also slowly fill, and the target life will be determined principally by the flushing of tritium by that portion of the deposited deuterium which does not go to zones 6, 7, and 8.

Thus we see that there are two modes of behavior: In one mode, where the energy density is high, the temperature pulse is sufficiently high for diffusion and surface transport to produce a higher "out" rate than the deposition or "in" rate. This mode results in "dumping" of the tritium inventory and short target life.

In the second mode, energy densities are low enough so that the deposition rate remains higher than the surface loss rate. Here the hydrogen-isotope inventory increases, and the target life is determined by the flushing rate of tritium by deuterium.

PARAMETRIC DESIGN STUDY

In order to further study the above two modes of target behavior, a series of TRUMP runs was made, based upon projected design parameters of higher rotating speed [576 rad/s (5500 rpm)], higher deuteron beam current (10 to 200 kW at 400 keV), and a larger target (140 mm radius).

Runs were made at the following conditions:

Beam profile, FWHM (mm)	Power (kW)
5	10-50
7.5	20-70
10	10-60
15	20-150
20	30-200

First, heat-flow mode runs were made to obtain temperature-time data (similar to Figs. 1 and 2). The results are plotted in Fig. 9. The maximum temperature rise for any beam size is directly proportional to the beam current.

The temperature-time profiles of the heat-flow runs were then used to calculate diffusivity-time and HSURE-time data for the mass-flow runs using TRUMP. The results of these runs are given in Fig. 10.

From Fig. 10 one can see that the mass flow of deuterium plus tritium from the target is enormously more sensitive to beam power than is the deposition rate

of deuterium into the target. In order to understand just how critical the operating parameters of Fig. 10 are, the study depicted in Fig. 11 was made. Here some rather naive conditions were assumed. The neutron-production-area zones (1 to 5) were lumped as a reservoir of tritium, ignoring the zones (6 to 8) behind the deuteron deposition zone (zone 5). The reservoir was treated as a dilution problem, with deuterium flow in and deuterium plus tritium flow out. This assumes instantaneous mixing, which the study of Davis and Anderson³ has shown to be in error. However, the half-tritium-inventory time as an estimate of target half-life should show how critical a factor

the relative flow rates are in affecting the half-life.

This study indicates that, when the rate out equals the rate in, the target half-life should be about 85 h (for 100 mm of radial target disk). If the rate in is twice the rate out, the half-life should be about 240 h (almost a factor 3 longer). If the rate in is half the rate out, the half-life should be about 35 h (almost a factor of 2.5 shorter).

If, now, we look at Fig. 10 for these same rates we see the relationships shown in Table 2.

If the power levels for $r_i = r_o$ are plotted on the temperature-rise plots of Fig. 9 (dashed line), we see that this

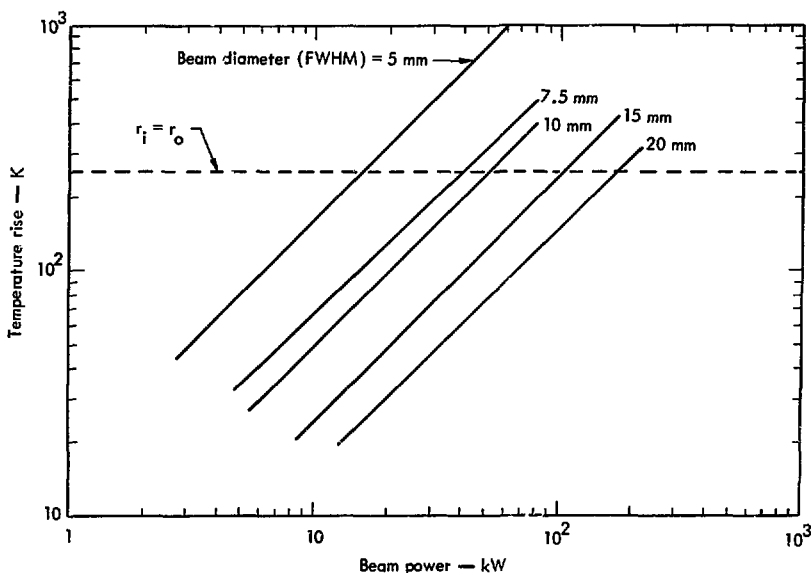


Fig. 9. Temperature rise of front face of TiH_2 for a 576-rad/s target (at 140-mm radius) as calculated with the TRUMP code.

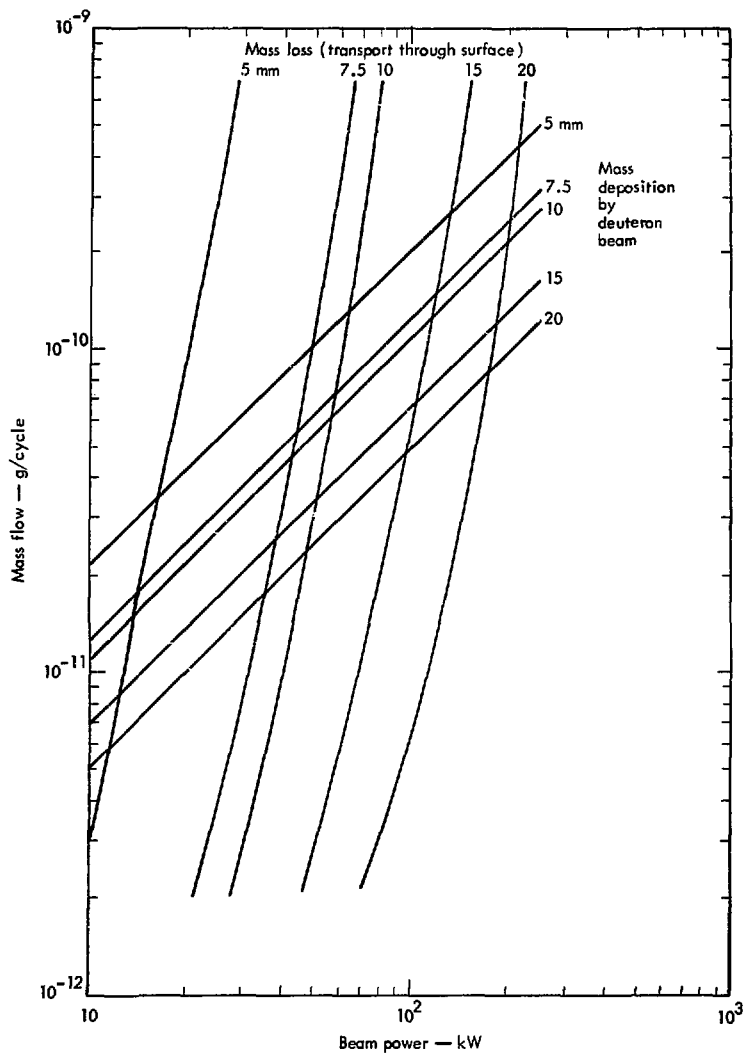


Fig. 10. Mass deposition and mass loss as functions of beam power at various beam diameters (FWHM).

operating condition corresponds to a constant temperature rise of the target front face of about 250 K. Since these calculations assumed an initial temperature

of 353 K, this, then, is a peak temperature of 603 K.

Increasing the input power by ~ 12% raises the front-face temperature and

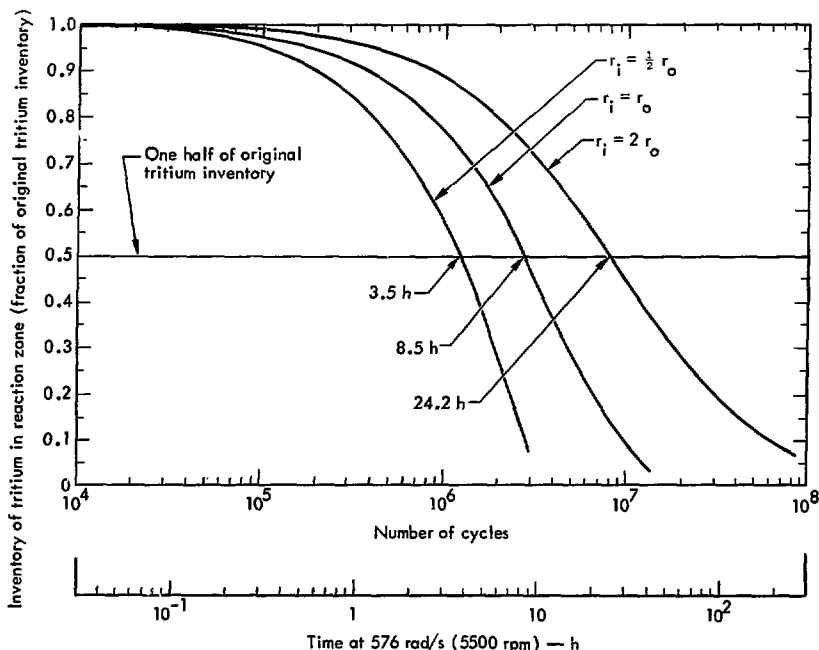


Fig. 11. Half-life of a 10-mm-wide disk on a 576-rad/s target as a function of r_i/r_o (based on a deposition rate of 5×10^{-11} g/cycle).

Table 2. Beam power at various ratios of rate in to rate out (see Fig. 10).

Beam profile, FWP (m)	Mass flow rate for $r_i = r_o$ (10^{-11} g/cycle)	Beam power (kW)		
		$r_i = r_o$	$r_i/r_o = 1/2$	$r_i/r_o = 2$
5	3.3	16	18	14
7.5	5.3	42	48	37
10	6.1	56	62	49
15	6.8	101	112	89
20	7.4	166	180	146

causes a decrease in half-life by about a factor of 3. This results in a total-target-life neutron output of $\sim 37\%$ ($1.12/3$) of the output at $r_i = r_o$.

Decreasing the input power by $\sim 12\%$ lowers the front-face temperature and results in a total-target-life neutron-output gain of 120% (0.88×2.5).

We thus see that the criterion of rate in equalling rate out seems to be a useful one for estimating operating parameters which yield the highest neutron-output rate consistent with a long half-life. Higher power exacts a disproportionate penalty in total neutron output over the useful half-life of the target.

Figure 12 is a plot of this relationship of beam width to beam power at the points where the rate in equals the rate out.

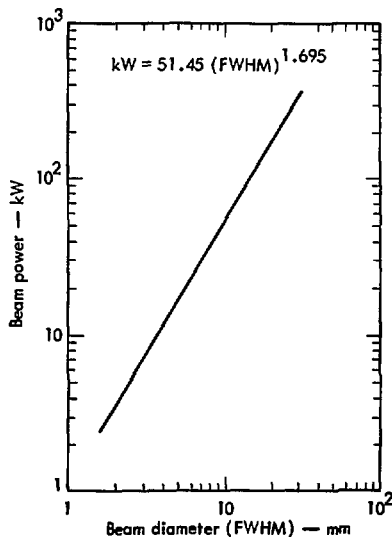


Fig. 12. Plot of points where $r_i = r_o$ (140-mm radius at 576 rad/s).

Conclusions

1. The relationships of Fig. 12 suggest the following:

a. Although there is no experimental evidence that operation of a target in a mode which continually increases the hydrogen-isotope content is destructive to the target, surely there is an upper limit to the hydrogen-isotope content of the gamma TiH_2 phase. This operational mode should be investigated by destructive examination of carefully overcharged targets by metallurgical techniques.

b. Both extremes of $r_i/r_o \gg 1$ and $r_i/r_o \ll 1$ seem to be poor operating parameters, and somewhere near $r_i/r_o = 1$ seems to be a useful designator

of proper operation. Instrumenting the ICT accelerator to continuously monitor target deuterium and tritium gas evolution, beam current, beam profile, and target front-face temperature should be useful to control optimum operating parameters in a closed-loop control mode.

2. The following facts suggest another useful alternative target design:

- a. Very little of the original tritium inventory is usefully converted to neutrons.
- b. The implanted deuterium sweeps the tritium out of the neutron conversion zone by dilution and diffusion, dumping it uselessly into the vacuum system.

c. The rate-controlling process is the surface reaction at the tritide-vacuum interface.

If the implanted deuterium could be deposited in a high-diffusion-rate material like palladium, it could be bled out of the target from behind the neutron-production layer rather than through the tritide layer.

The tritium of the tritide layer could be prevented from diffusing through the surface layer to the vacuum system, or through the tritide-palladium interface, by a suitable hydrogen-isotope diffusion barrier.

This technique has already been suggested in the literature.⁵ The work

reported by Sandia⁴ suggests that the TiO_2 or TiN barrier layers *might not* be satisfactory. This approach to target design should be investigated to determine optimum materials and thicknesses.

The simplicity of this approach, and the huge potential target-life increases implicit in it, indicate a very fruitful return for a modest effort.

Such a "captured-tritium" target might not have the limitations of the approach suggested in conclusion 1 above, but it surely would have other operational limits, probably based on stability or damage to the diffusion-barrier layers. These, too, would have to be investigated.

References

1. R. Booth and H. H. Barschall, Nucl. Instr. Methods 99, 1 (1972).
2. C. M. Logan, A Model for Tritium and Deuterium Transport in Targets for Neutron Generators, Lawrence Livermore Laboratory, Rept. UCRL-51634 (1974).
3. J. C. Davis and J. D. Anderson, Tritium Depth Profiling by Neutron Time-of-Flight, Lawrence Livermore Laboratory, Rept. UCRL-75757 Preprint (1974).
4. C. W. Schoenfelder and J. H. Swisher, "Kinetics of Thermal Decomposition of TiH_2 ," J. Vac. Sci. Technol. 10, No. 5 (September/October 1973).
5. Long Life Neutron Generator Target Using Deuterium Pass-Through Structure, NASA Technical Brief B74-10063 (July 1974).